

# Spaceborne to UAV Bistatic Radar System for High-resolution Imaging and Autonomous Navigation

Marc Rodriguez-Cassola, Marwan Younis, Gerhard Krieger  
Microwaves and Radar Institute, German Aerospace Center (DLR), 82234 Wessling, Germany

Michael Oswald  
Astrium GmbH Satellites, Military Programs, 88039 Friedrichshafen, Germany

Luca del Monte  
European Space Agency, Security Strategy and Partnership Development Office, 75738 Paris, France

## Abstract

Bistatic radars offer several advantages when compared to their monostatic counterparts. In addition to increased performance, sensitivity, coverage and revisit times, all of them parameters which are mainly dependent on their spatial configuration, bistatic radars offer the objective advantage of being more robust to jamming, since the receiver operates as a mere passive system. The proposed system consists of a spaceborne radar transmitter illuminating an area of interest and one or several radar receivers mounted on a UAV to perform a two-goal mission: a) help autonomous navigation of the UAV by performing the sense and avoid function, and b) perform surveillance of the overflow area using high-resolution remote sensing techniques. Although the requirements for these significantly different tasks might seem distant, having a spaceborne transmitter ensures that the coverage needed for both purposes is achievable. The system can provide a cheap and robust manner for enabling global UAV flight, while enabling continuous all-weather imaging capabilities.

## 1 Introduction

The feasibility of high-resolution spaceborne-airborne bistatic remote sensing has been recently shown in a series of experiments carried out between the German satellite TerraSAR-X and DLR's F-SAR [1]. A significant improvement in terms of SNR and resolution with respect to the spaceborne monostatic system was achieved, mainly because of the shorter ranges between the receiver and the scene. Since a SAR is in nature a regular range-Doppler radar, the transmitter signal can also be used to implement a bistatic tracking radar to survey the surroundings of the airplane. Provided that the UAV keeps its nominal track, autonomous navigation can be split into two main tasks: a) sense and track the surrounding flying objects, and b) avoid these flying objects in case the trajectories of the two airplanes collide. The sense and tracking capabilities of the radar can be quantified with measures of range and Doppler resolutions and the sensitivity of the system [2]. This paper analyses the suitability of a space-based bistatic radar for allowing remote sensing and autonomous navigation of a UAV platform. As expected, the presented system shows a different character with respect to remote sensing and sense and avoid requirements, since persistent coverage opposes to high SNR observations.

## 2 System requirements

Depending on the selected orbits, the usual trade-off between coverage, repeat cycles and number of satellites can be established. The fixed characteristics on the UAV flight and dimensions are listed in Table 1.

**Table 1:** UAV characteristics

Velocity [km/h]	[50, 1000]
Height [km]	[0.15, 25]

The requirements for the remote sensing subsystem are listed in Table 2. These values are derived from realistic values of spaceborne and airborne remote sensing systems.

**Table 2:** Remote sensing requirements

Geometrical resolution [m]	5
NESZ [dB]	-20
Revisit times [h]	48
Scene size [km×km]	$2 \times 2 \text{ km}^2$

The requirements for the sense and avoid subsystem are listed in Table 3.

**Table 3:** Sense and avoid requirements

Range [km]	27
Bistatic RCS [m <sup>2</sup> ]	> 1
Information update period [s]	1
Information delay [s]	0.5
Coverage region (height difference) [m]	±500
Target velocity range [km/h]	[0, 1000]

## 3 General assumptions

On one hand, using a LEO satellite as transmitter improves the overall performance of the system, mainly because the transmitter is closer to the scene. On the other hand, sense and avoid function requires persistent monitoring of the

area where the UAV is flying, which mixed with LEO condition, results in a constellation with an enormous amount of satellites. If persistent monitoring is desired, MEO-orbit satellite constellations are needed. The previous two conclusions summarise the character of the system. Achieving high resolution, high SNR radar images with a MEO constellation guaranteeing constant monitoring in higher frequency bands requires very expensive bandwidths and transmitted powers. Likewise, realistic configurations allowing high resolution and high SNR images [1] cannot guarantee persistent monitoring, and thus are not able to perform the sense and avoid task. Since the MEO solution allows both sense and avoid and remote sensing, whereas the LEO solution only allows remote sensing, we retain as proposed system a MEO constellation guaranteeing persistent coverage of the interesting areas. Sense and avoid range and velocity range conditions fix the first parameter of the system. If classical time-frequency limitation of range-Doppler radars for unambiguous target localisation is considered, the carrier frequency has to be strictly under 6 GHz. The PRF is then bounded to a maximal value of 11 kHz. Since we aim to push the resolution of the system for imaging purposes, the carrier should also be as high as possible. Therefore, C-band is the selected frequency band of the system. Accepting a carrier frequency range between 5 and 6 GHz, the PRF varies between 9.25 and 11 kHz. Ideally, the system consists of a C-band MEO satellite constellation illuminating with chirp pulses the interesting areas. These pulses are used for both purposes, and so no further intelligence on the transmitter part needs to be included. Ideally too, the receiver is mounted on the UAV and is shared for remote sensing and sense and avoid (the ideally is to be understood as a to be desired, since further analysis on timing and clutter should be performed to ensure the previous statement and therefore this might not be feasible in a final system), and separate antennas are used for remote sensing and sense and avoid. A central unit should in that case be responsible for the time allocation of the receiver to the different subsystems. An integrated positioning unit (usually IMU + GPS) is essential for absolute location of the targets detected by both subsystems. Receiver remote sensing antennas have to be designed so that image NESZ is better than  $-20$  dB, provided that transmitted power, pulse duration and transmitter antenna gain have already been optimized (and fixed) for the satellites. The antennas are side-looking, the only sensible solution for such a system, if acceptable resolution imaging is desired. For imaging a given area, the UAV will flow side-looking to it. Receiver sense and avoid antennas are distributed all around the UAV to guarantee  $360^\circ$  surveying of the airplane environment. A scanning on the azimuth plane of the antennas is proposed, and thus the azimuth beamwidth of the antennas is a function of the desired gain and of the properties of such a scanning. The elevation beamwidth depends on the desired gain and on the relative height coverage requirement of the system. Two realistic system examples are presented in the following section.

Both solutions use a MEO constellation and have different coverage areas. The first one consists of a reduced Galileo-like (15 satellites) constellation allowing persistent global coverage, the second one is a lower-orbit MEO constellation (5 satellites) allowing persistent coverage of the polar regions. Both yield remote sensing performance comparable to state-of-the-art radar imaging satellites, showing the advantage of the system. Regarding all the previous considerations, the reference system which will be used for the system examples and performance analysis is presented in Table 4.

**Table 4:** Reference System Parameters

Orbit height [km]	25000/13300
Carrier frequency [GHz]	5.405
Transmitted bandwidth [MHz]	100
Transmitted peak power [kW]	10/5
Duty cycle [%]	20
Satellite incident angle range [deg]	[0, 60]
Antenna size (Tx)	15 m parabolic
RS antenna size (Rx)	0.312 m <sup>2</sup>
SA antenna size (Rx)	> 0.0312 m <sup>2</sup>

## 4 System examples

### 4.1 MEO constellation for global coverage

The constellation has three orbital planes and only 5 satellites per plane, all of them in relative positions of Walker Delta pattern  $56^\circ:27/3/1$ . The orbit height is 25000 km. Using this configuration, the number of satellites needed is 15. Figure 1 shows a snapshot of the density of satellites illuminating the Earth regions.

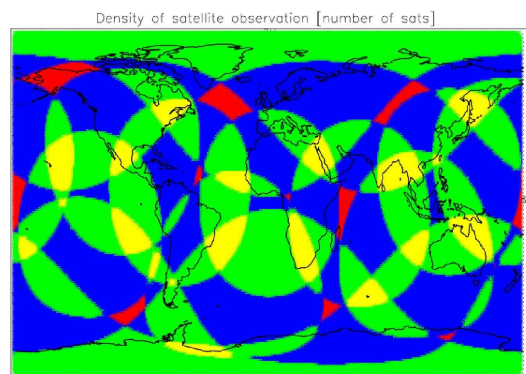


**Figure 1:** Density of satellites illuminating the Earth at a given instant. 1 satellite (red), 2 (blue), 3 (green), and 4 (yellow).

#### 4.1.1 Performance of the remote sensing subsystem

**Resolution:** Using the 100 MHz transmitted bandwidth of the reference system, the range resolution analysis is presented in Fig. 2. In the figure, we can see the percentage

of the Earth which is imaged with a determined range resolution for backward- (left) and forward-scattering (right) cases computed at the mid-beam point of the UAV antenna. The worst resolution in the right plot case has to be understood as the best of the worst, since range resolution may not be bounded for the forward-scattering case. Note that in both cases, the majority of the Earth is imaged with the best possible range resolution. Range resolutions better than 5 m occur in 99% of the backward-scattering cases and almost 55% of the forward-scattering cases.

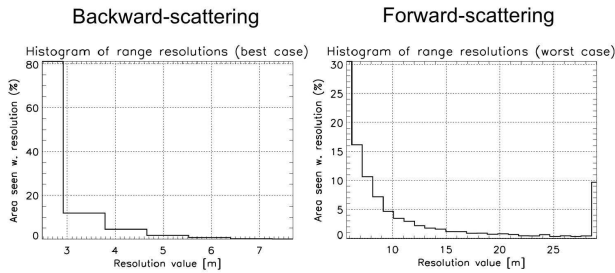


**Figure 2:** Percentage of the Earth imaged with given range resolution for backward- (left) and forward-scattering (right).

Considering the synthetic resolution, Fig. 3 (left) shows the length of the synthetic aperture required for the system to achieve a synthetic resolution of 5 m as a function of the UAV height. As expected higher UAV flight heights require longer synthetic apertures. The corresponding integration times remain below 8.5 s for a UAV speed of 100 m/s, which is within the range of what is currently achievable with state-of-the-art airborne SAR systems.

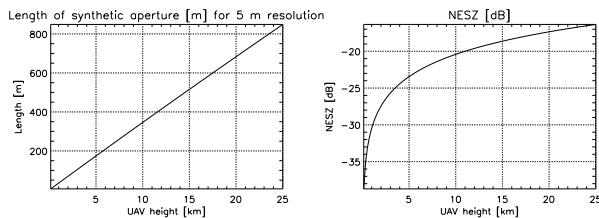


**Figure 3:** Length of the synthetic aperture required for achieving a synthetic resolution of 5 m (left). NESZ (right).

**Sensitivity:** The sensitivity analysis is performed assuming a resolution cell of  $5 \times 5 \text{ m}^2$ . The transmitted peak power with respect to the reference system is 10 kW. The NESZ values are shown in Fig. 3 (right). We observe that NESZ depends inversely on UAV height, since for all cases the synthetic resolution is kept constant. The requirement is fulfilled for heights under 11 km.

#### 4.1.2 Performance of the sense and avoid subsystem

**Resolution:** The resolution analysis for the sense and avoid subsystem is rather general and independent of the

constellation. Fig. 4 shows the plots corresponding to range (left) and Doppler (right) resolution analysis. The left plot shows the maximum bistatic angle as a function of the transmitted bandwidth and of the desired range resolution. Note that this resolution degrades when targets approach to the baseline vector of the bistatic radar, which is an intrinsic property of bistatic radars themselves. For the 100 MHz considered case, and assuming a range resolution of 5 m, the maximum bistatic angle takes a value slightly over  $150^\circ$ . The right plot on the other hand shows the speed resolution for an extended PRF range and integration times below 0.5 s. We see that integration times over 0.1 s already yield resolutions under 1 m/s, largely sufficient for the foreseen task.

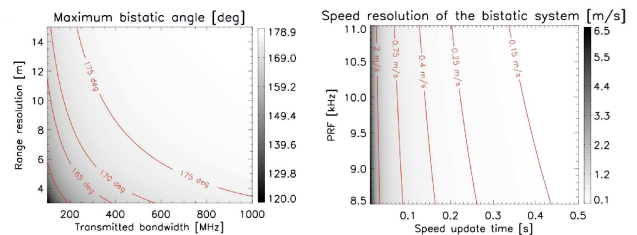


**Figure 4:** Range resolution (left) and Doppler resolution (right) analysis for the sense and avoid subsystem.

**Sensitivity:** The SNR values after coherent processing of the target echoes (for an integration time of 0.1 s) and as a function of the satellite off-nadir angle are shown in Fig. 5 (left). Even for the small RCS of the target, its signature is expected to be detected on the radar. Moreover, having an integration time of 0.1 s allows to achieve an azimuth angular resolution of  $36^\circ$  using a single receiver.

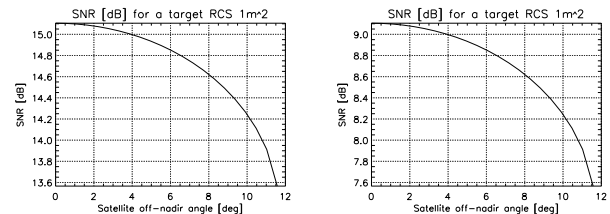


**Figure 5:** SNR after coherent integration for a target with a bistatic RCS of  $1 \text{ m}^2$  for an integration time of 0.1 s. Global coverage case (left) and polar coverage case (right).

## 4.2 MEO constellation for polar coverage

The constellation consists of 5 satellites in a single orbital plane. The orbit height is 13300 km, with an inclination of  $89.5^\circ$ . This orbit height could be affected by the outer Van Allen radiation belt, which might pose problems to the selection of this constellation for a final design. Since its use does not change significantly the results and conclusions of the study, we retain the example for its illustrative

value. We nonetheless remind that a realistic constellation should be placed at a 1000 to 2000 km lower orbit. The deviations in performance would favorise the lower orbits when compared to the ones shown in this case. The proposed constellation guarantees persistent coverage of the polar regions, above  $66.55^\circ$  latitudes North and South, respectively. Figure 6 shows a snapshot of the density of satellites illuminating the Earth regions (right).

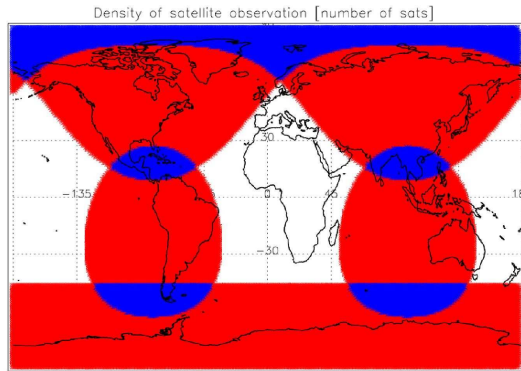


**Figure 6:** Density of satellites illuminating the Earth at a given instant: 0 satellites (white), 1 (red), and 2 (blue).

#### 4.2.1 Performance of the remote sensing subsystem

**Resolution:** The same analysis as the one shown in 4.1.1 for the range resolution has been performed. The results are shown in Fig. 7. Since the incident angle range is exactly the same as the one of the previous constellation and due to the, in general, lesser number of satellites with which a given area is imaged, the flexibility of the constellation to yield a better bistatic configuration is lower than for the constellation for global coverage case. Therefore, the results are also a bit worse than those shown in Fig. 2. The tendency is however the same, being the majority of the covered area imaged with the best available range resolution.

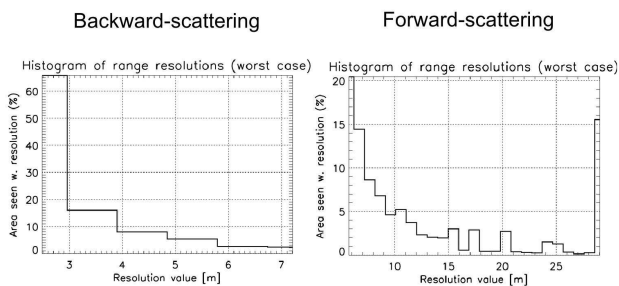


**Figure 7:** Percentage of the Earth imaged with given range resolution for backward- (left) and forward-scattering (right).

The synthetic resolution analysis, similar to the one of 4.1.1, is shown in Fig. 8 (left). The required lengths of the synthetic aperture do not change much, since synthetic resolution is mainly achieved by the motion of the UAV.

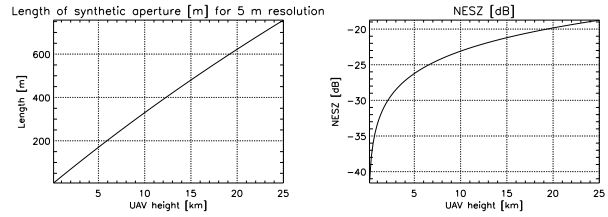


**Figure 8:** Length of the synthetic aperture required for achieving a synthetic resolution of 5 m (left). NESZ (right).

Like in the case of the global coverage constellation, the corresponding integration times are below of 7.5 s for 25 km UAV flight height. Similar integration times are not uncommon in present airborne SAR systems.

**Sensitivity:** The same resolution cell of  $5 \times 5 \text{ m}^2$  is used for the sensitivity analysis of this constellation. The transmitted peak power with respect to the reference system is 5 kW. The NESZ values as a function of UAV height are shown in Fig. 8. The dependence of NESZ with UAV height is also linear, like in Fig. 3. The requirement is fulfilled for all almost UAV heights. As expected, more reasonable transmitted peak powers are obtained if only partial, though persistent, coverage is required.

#### 4.2.2 Performance of the sense and avoid subsystem

**Sensitivity:** The SNR values after coherent processing of the target echoes (for an integration time of 0.1 s) are shown in Fig. 5 (right).

## 5 Summary

A space-based bistatic radar with a dual character has been presented. The same transmitter is used by two subsystems mounted on a UAV to perform two different tasks: a) high-resolution imaging of interesting overflown areas, and b) help autonomous navigation of the UAV. Some requirements for the system performance and operation have been derived and two exemplary systems with different coverage regions have been designed. The first one allows persistent coverage of the Earth with a 15-satellites Galileo-like constellation. The second one, with 5 satellites placed on a lower orbit, allows persistent coverage of the polar regions. This study was funded by ESA Contract no 22448/09/F/MOS.

## References

- [1] M. Rodriguez-Cassola *et al*, 'Bistatic TerraSAR-X/F-SAR spaceborne-airborne SAR experiment: description, data processing and results', *IEEE Trans. Geosci. Remote Sens.*, vol. 48, no. 2, pp. 781-794, Feb. 2010.
- [2] G. Krieger *et al*, *Analysis of system concepts for bi- and multi-static SAR missions*, Proceeding of IGARSS, 2003, Toulouse, France.